Nonlinear effective barriers for flux diffusion and critical current density of $HgBa_2Ca_2Cu_3O_x$ based upon ac susceptibility measurement

S. Y. Ding, J. Li, and H. M. Shao
Department of Physics and Center for Advance Studies in Science and Technology of Microstructures, Nanjing University, Nanjing 210093, People's Republic of China

J. W. Lin
Department of Math and Physics, Hohai University, Nanjing 210098, People's Republic of China

C. Ren and X. X. Yao
Department of Physics and Center for Advance Studies in Science and Technology of Microstructures, Nanjing University, Nanjing 210093, People's Republic of China

(Received 3 January 1995)

The complex ac susceptibility of $HgBa_2Ca_2Cu_3O_x$ was measured systematically as a function of temperature T, ac field amplitude, frequency, and dc field H_d to study the flux dynamics in a time window of 10^{-5}–10^{-2} s. The dependences of the effective barriers for flux diffusion U on current density J, $U \propto J^{-\mu}$, as well as H_d and T were determined. The rate of current relaxation $J(t)$, E vs J curves, and the so-called irreversibility line were deduced from U. The critical current density J_c as a function of T and H_d was estimated. $\mu = 0.43$ is close to 0.5, one of the glassy exponents predicted by the vortex glass and collective creep theories. The high and stable $J_c(H_d, T)$ and the highest T_c indicate that the Hg-based superconductor is a promising material for technical applications.

I. INTRODUCTION

The facts that T_c of $HgBa_2Ca_2Cu_3O_y$ (Hg-1223) is higher than 130 K and its structure is similar to that of the toxic $TlBa_2Ca_2Cu_3O_x$ (Tl-1223), which has strong flux pinning and less anisotropy, make studies on the flux dynamics and critical current density J_c for this superconductor rank among the most interesting research subjects.[1–9] However, the usual relaxation experiments using conventional magnetometers are restricted to instrumental integration times (larger than a few seconds). This precludes getting information occurring at earlier times. The ac susceptibility (ACS) technique is a powerful tool for these studies not only for its convenience but also for the quick response, which is typically in a time window of 10^{-5}–10^{-1} s (10^5–10 Hz).[10–12] Among flux dynamics studies, determination of the effective barrier for flux diffusion is fundamental. It is the main goal of this work to study nonlinear flux dynamics, i.e., current-dependent barriers, current relaxation, and the E vs J $[E(J)]$ curve, etc., predicted by the vortex glass and collective creep theories.[13,14] We use ACS measurements in the millisecond time window.

Consider a sample of a thin slab with applied field $H \| Z$, $J \| Y$, and $v \| X$, thickness $2d$, $x = 0$ at the center of the slab, where v is the flux velocity. The nonlinear flux diffusion equation is

$$\mu_0 \partial_t J - \partial_x^2 [b v_0 e^{-U(J)/T}] = 0, \tag{1}$$

where b is the local induction, $v = v_0 e^{-U(J)/T}$ $[v_0 = v(U=0)]$. This highly nonlinear equation has been solved theoretically.[12] The activation barriers are

$$U[J(t), H_d, T] = T \ln(1 + t/t_0) \tag{2}$$

with time scale $t_0 = Td^2/(2H_d v_0 |\partial_J U|)$. The flux creep governed by Eq. (2) results in a space- and time-dependent screening current. The decay of the current density leads to an increase in the barrier whereas in the opposite case $\delta J > 0$ the barrier decreases. The dynamical behavior of the system then tends to eliminate all the fluctuations in the system such that the current density J and hence $U(J)$ becomes constant throughout the sample. So the straight-line approximation (the ''Bean critical state'') provides a good description of the field profile inside the sample.[12]

In an ACS experiment with large ac fields such that the vortices diffuse nonlinearly this critical state decay competes with the time scale $t = 1/f$ imposed on the system by the external ac field. In this case the decay of the magnetization occurs on the time scale t such that the screening currents flowing in the sample are given by $U(J) = T \ln[1 + 1/(ft_0)]$. The current density is $J = U^{-1}[T \ln\{1/(ft_0)\}]$ $(ft_0 \ll 1)$ instead of being the critical value J_c due to the diffusion of vortices. Accordingly, the penetration depth of the vortices is given by $\delta = h/J$ and depends also upon temperature, frequency, and dc field. The χ'' peaks when the flux front reaches the center of the sample, i.e., $\delta = d$, because, say, the temperature reaches T_p, the peak temperature of the imaginary part of the ACS. The criterion for the peak in χ'' is[11–12]

$$U[J(T_p), H_d, T_p] = T_p \ln[1/(ft_0)], \tag{3a}$$

$$J[T_p(f)] = h/d, \tag{3b}$$

with $t = 1/f$. Equations (3) determine the barrier and current density, as in dc magnetization decay measurements. Thus it is possible to measure the current-dependent activation bar-

rier by studying the position of the peak in $\chi''(T)$ for different f, h, and H_d. From the barrier U the relaxation of current and the characteristic $E(J)$ curves can be determined as well.

The critical current density is another important parameter. Due to the difficulties of transport measurements for ceramic samples, hysteresis loops and ACS methods have been widely used to study the magnetic J_c. In the two methods a static critical state model such as the Bean model is invoked. J_c in the ACS method is[15–18]

$$J_c(T_p)=h/d. \tag{4}$$

Nevertheless, the giant flux creep means current decay and is a severe challenge for the static model for estimating J_c. The J_c estimated from Eq. (4) should be frequency independent, otherwise it is not proper. A method for extracting the critical current from the frequency-dependent ACS data would be interesting. On the other hand, it has been shown that there exists a true superconducting J_c in the vortex glass phase[13] because the effective barrier for flux creep increases without limit with decreasing current density. The other goal for this work is how to find such a J_c for Hg-1223. Also, we will estimate the J_c value as a function of dc field and temperature assuming a special criterion for the ACS technique.

In this paper we report systematic measurements of the real (χ') and imaginary (χ'') parts of the ACS as a function of temperature in different ac field amplitudes, frequencies, and dc fields, and the flux dynamics properties of Hg-1223 in the time window 10^{-5}–10^{-2} s (10^5–10^2 Hz).

II. EXPERIMENTS

The sample was synthesized as follows. The precursor material with a nominal composition $Ba_2Ca_2Cu_3O_x$ was prepared by calcining a thoroughly mixed powder of appropriate amounts of BaO_2, CuO, and CaO at 900 °C for 24 h. These precursors were then mixed with HgO_2, pressed into pellets, sealed in evacuated quartz tubes, and heated in a closed steel container for 8 h at 600–800 °C. A relatively slow heating rate (1 °C/min) between 400 and 600 °C, where HgO decomposes, was needed to avoid explosion of the quartz tube. Details of sample synthesis and characterization have been given elsewhere.[8]

The complex ACS was measured in a home-made ac susceptometer with sensitivity of 10^{-8} emu at different frequencies, amplitudes, and dc fields in the applied field $H(t)=H_d+h\cos(2\pi ft)$ where $H_d \gg h$ or $H_d=0$. All the data for $\chi(T)$ were recorded by a computer for later analysis.

III. RESULTS AND DISCUSSIONS

A. The effective barrier *U*

Shown in Fig. 1 is the temperature dependence of χ' and χ'' for the sample at $H_d=0$, $h=0.2$ G, and $f=1.5$ kHz. From Fig. 1 one can find only one χ' step with onset at $T_{c0}=133$ K and one χ'' peak at $T_p=125$ K. In order to go further into the flux dynamics, we measured the ACS as follows. First, we measured $\chi(T)$ at varying frequencies f_k ($k=1,2,3,...$), fixed H_{dj}, and fixed h_i to obtain the influence of f on the χ'' peak temperature, $T_p(f_k)$, which is used to extract $U(T_p)$. Then we changed H_{dj} and h_i ($i,j=1,2,3,...$) and measured $\chi(T)$ to obtain $T_p(h_i,H_{dj},f_k)$ in the same way, which are used to

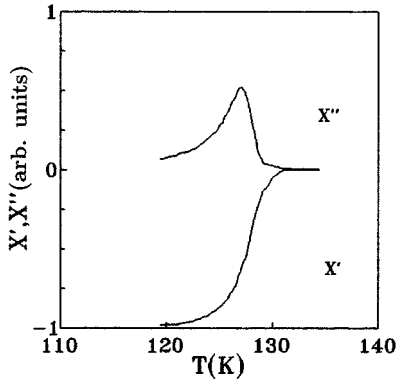

FIG. 1. χ' and χ'' as a function of temperature at $H_d=0$, $f=1.5$ kHz, and $h=0.02$ G.

extract $U(J,H_d,T_p)\equiv U_0(J,H_d)U(T_p)$. As an example of $T_p(f_k)$, Fig. 2 shows the temperature dependence of χ'' for different frequencies f_k at $H_d=3$ kG and $h=0.36$ G, where one can see that T_p increases with increasing f, and hence we have obtained $T_p(f_k)$. This $T_p(f_k)$ of Fig. 2 is also illustrated in Fig. 3 by open squares which are fitted by the solid straight line labeled 4 but in a different way, i.e., a plot of $U(T_p)/T_p$ versus f with $U(T_p)\equiv[1-(T_p/T_c)^r]^n$ and $T_c=117.1$ K. Adjusting the r and n, we find that when $r=2$ and $n=2$ in the temperature regime $T_{p_{\max}}-T_{p_{\min}}\approx 20$ K the fitting functions are straight lines described by the Arrhenius law[16–18]

$$U(T_p)/T_p=[U_{04}(h,H_{d4})]^{-1}\ln[1/(ft_{04})], \tag{5a}$$

where $\ln(1/t_{04})$ and $[U_{0j}(h,H_{dj})]^{-1}$ are the intercept and the slope of the fourth fitting line, respectively. Displayed in Fig. 3 are summaries of the data (symbols), showing the effect of dc fields on slopes and intercepts of the fitting straight lines. It is found that $\ln(1/t_{0j})$ only varies slightly with H_{dj} and has mean value $1/t_0\approx 10^9$ Hz from the seven intercepts. Plotting $U_{0j}(h,H_{dj})$ versus H_{dj} (Fig. 4), we find that a function well fitting the seven slopes is[16–18]

$$U_0(H_d)=U_{0h}H_d^{-m} \tag{6}$$

where $m=1$. Therefore Eq. (5a) is the experimental fitting equation:

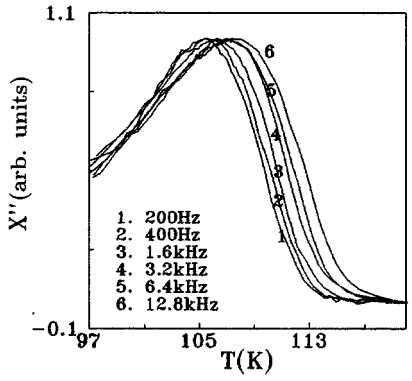

FIG. 2. χ'' as a function of temperature at $h=0.36$ G and $H_d=3$ kG at different frequencies.

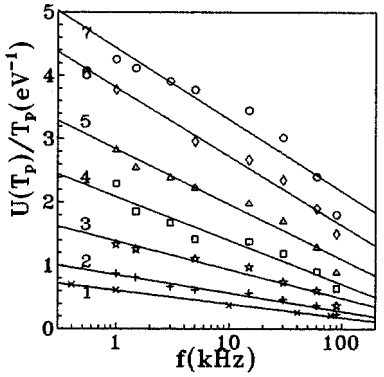

FIG. 3. The plot of $U(T_p)/T_p$ $[=(1-T_p^2/T_c^2)^2/T_p]$ versus f in different dc fields H_d (1, 1 kG, 2, 1.5 kG, 3, 2 kG, 4, 3 kG, 5, 4 kG, 6, 5 kG, and 7, 5.9 kG). $h=0.36$ G. The solid straight lines are fitted curves.

$$U(T_p)U_0(h,H_d)=T_p\ \ln[1/(ft_0)]. \tag{5b}$$

It is easy to see from Eq. (3b) that U_{0h} is in fact U_{0J} which can be determined by a measurement similar to that for $U_0(H_d)$ but at different h_i. This measurement has been done: an example of the effect of h on the χ'' peak, $T_p(h_i)$, is shown in Fig. 5(a) and the data (symbols) are summarized in Fig. 5(b) where the fitting functions are the straight lines whose slopes are just U_{0hi}. Plotting these U_{0hi} versus h_i and using Eq. (6), we obtain the fitting function (solid curves in Fig. 6)

$$U_0(J,H_d)=AJ^{-\mu}H_d^{-m} \tag{7}$$

where $\mu=0.43$ and A is a constant. For the case $H_d\geqslant 1$ kG, the sample size $2d$ is considered to be the grain size. Scanning electron microscopy observation shows the average grain size is about 2 μm ($d=1$ μm) from which $A=2.4\times10^9$ $(\mathrm{A/cm^2})^{\mu}\,\mathrm{G}^m\,\mathrm{K}$. To compare with magnetization relaxation and hysteresis loop experiments where J is of the order of 10^6 A/cm^2, we extrapolate Eq. (7) and have $U_0\equiv U(J=10^6$ A/cm^2,$H_d=20$ kG,$T_p=0$ K$)\approx 10$ meV. This value is comparable with the other high-T_c superconductors. Substituting Eq. (7) and $U(T_p)$ into Eq. (5b), we have

$$AJ^{-\mu}H_d^{-m}[1-(T_p/T_c)^r]^n=T_p\ \ln[1/(ft_0)], \tag{8}$$

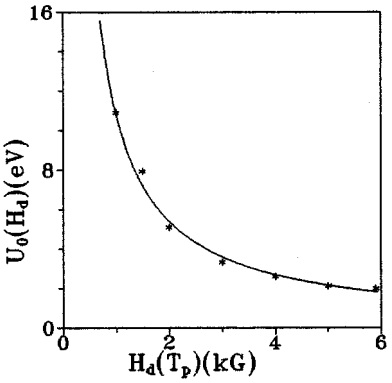

FIG. 4. $U_0(H_d)$ $[=U(h=0.36$ G, H_d, $T=0$ K$)]$ as function of dc field [*: the slopes of the lines in Fig. 3; solid lines: $U_0(\mathrm{eV})=10.7/H_d(\mathrm{kG})$].

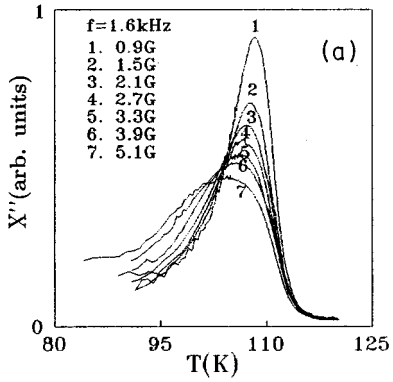

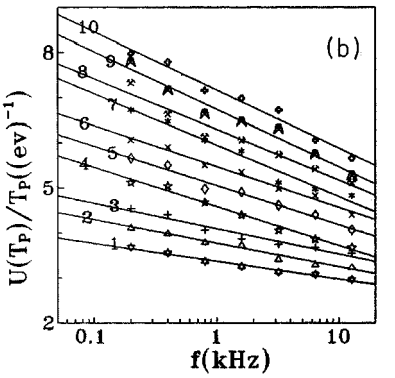

FIG. 5. (a) χ'' as a function of temperature at $H_d=3$ kG in different ac amplitudes shown in the figure. (b) The plot of $U(T_p)/T_p$ $[=(1-T_p^2/T_c^2)^2/T_p]$ versus f at different amplitudes h (1, 0.3 G, 2, 0.6 G, 3, 0.9 G, 4, 1.5 G, 5, 2.1 G, 6, 2.7 G, 7, 3.3 G, 8, 3.9 G, 9, 4.5 G, and 10, 5.1 G). $H_d=3$ kG. The solid straight lines are the fitted curves.

which has the characteristic predicted by the vortex glass and collective creep theories.[12–14] Noting that $T_p\geqslant 100$ K and $J\leqslant 10^3$ A/cm^2, we consider $\mu=0.43$ to be evidence that the flux system is in the charge-density-wave-type pinning and creep regime where the two theories predict $\mu=0.5$. Equation (8) is fundamental for nonlinear flux dynamics as discussed below.

B. The irreversibility lines

It is very easy to find the so-called irreversibility lines (IL's). From Eq. (8) we have (at given f and h)

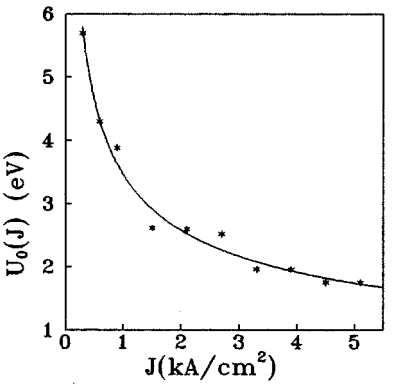

FIG. 6. $U_0(J)$ $[=U(J,\ H_d=3$ kG, $T_p=0$ K$)]$ as a function of J (*: the slopes of the lines in Fig. 5(b); solid line: $U_0(\mathrm{eV})=3.46[J(\mathrm{kA/cm^2})]^{-0.43}$).

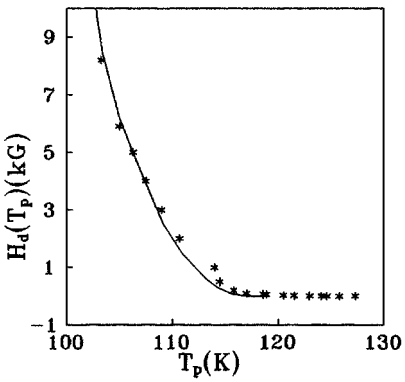

FIG. 7. The irreversibility lines $H_d(T_p)$. $f=1.5$ kHz. $h=0.2$ G. Solid line: Eq. (9). Symbols: data from Fig. 3 for $f=1.5$ kHz.

$$H_d(T_p)=C(J,f\,)[U(T_p)/T_p]^{1/m} \tag{9a}$$

which becomes (near T_c)

$$H_d\approx C_1(J,f\,)(1-T_p/T_c)^{2/m}/T_p^{1/m} \tag{9b}$$

where $C=\{A^{-1}J^{\mu}\ln[1/(ft_0)]\}^{-1/m}$ and $C_1=4C$. Equation (9) shows that the IL's are dependent not only on the irreversibility (the barrier U) of the sample but also on ac frequency, amplitude, and sample size (t_0), and thus are not an intrinsic material property. An example of the IL's described by Eq. (9) is shown in Fig. 7 ($f=1.5$ kHz and $h=0.2$ G) by the solid curve. It should be emphasized that Fig. 3 represents IL's measured at different frequencies f_k for given h. To every f_k there corresponds a different IL as shown by the data shifted vertically, e.g., the IL shown in Fig. 7 by the symbols is constructed from the data for $f=1.5$ kHz in Fig. 3. One can also construct another sort of IL at different ac amplitudes h with fixed f. Therefore one should be careful when one compares the present IL's with those obtained from different measurements and samples. For example, a dc magnetic method may be equivalent to the ACS one as $f\rightarrow 0$ whereas an electric transport experiment is similar to the ACS one at small J and very high frequencies ($t\rightarrow 0$).

C. The current density J

It is easy to obtain the current density from Eq. (8):

$$J=\{AH_d^{-m}U(T_p)/[T_p\ \ln(1/ft_0)]\}^{1/\mu}. \tag{10a}$$

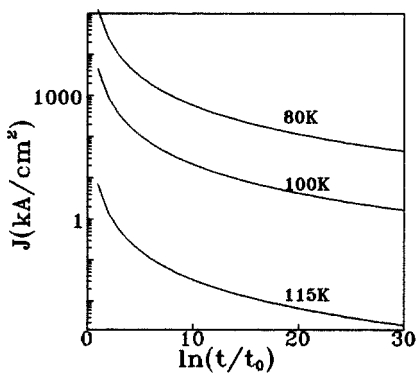

FIG. 8. The current relaxation $J(t)$ at $H_d=3$ kG and different temperatures.

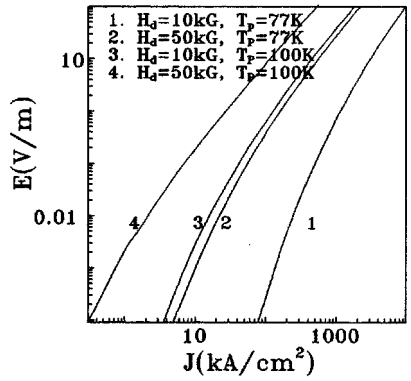

FIG. 9. The characteristic $E(J)$ curves at different fields and temperatures.

Since $t=1/f$, $J(f\,)$ is in fact the current relaxation equation:

$$J=\{AH_d^{-m}U(T_p)/[T_p\ \ln(t/t_0)]\}^{1/\mu}. \tag{10b}$$

Figure 8 displays the curve $J(t)$ described by Eq. (10). This ACS measurement is performed in the time window of $9\leqslant\ln(t/t_0)\leqslant 18$ ($10^{-5}\leqslant t\leqslant 10^{-1}$ s) whereas the range for the usual dc magnetic relaxation is $20\leqslant\ln(t/t_0)\leqslant 30$ ($10\leqslant t\leqslant 10^4$ s) and for electrotransport is $\ln t/t_0<5$.

From Eq. (10b) the normalized relaxation rate $S\equiv -d\ln J/d\ln t$ is $1/[\mu\ln(t/t_0)]$. It is clear that S is independent of temperature, and is 0.03 for $t=10^{-3}$ s ($f=1$ kHz) and 0.017 for $t=10^3$ s ($f=1$ mHz), the so-called ''plateau'' as observed in $YBa_2Cu_3O_y$.[19]

D. The $E(J)$ curves

We now switch off the ac field to study the electric field E induced by the current relaxation. According to the London equation this electric field is

$$E=-\mu_0 d^2\partial_t J, \tag{11a}$$

where d is the penetration depth at the χ'' peak. Using Eq. (10b), we have

$$E=\mu_0 d^2 J^{1+\mu}\ \exp[-(J_g/J)^{\mu}]/(\mu J_g^{\mu}t_0) \tag{11b}$$

where $J_g\equiv\{AH_d^{-m}[(1-T_p^2/T_c^2)^2/T_p]\}^{1/\mu}$. Equation (11b) shows that E decays with decreasing J exponentially, as predicted by vortex glass theory, and there indeed exists ''zero resistance current'' in Hg-1223 for a given E_c.[12] Shown in Fig. 9 are the $E(J)$ curves according to Eq. (11b) at $f_0=10^9$ Hz ($t_0=10^{-9}$ s) and several temperatures and fields.

E. Critical current density

From Eq. (11b) we can obtain J_c as a function of temperature and dc field for a given criterion E_c:

$$J_c=[\mu t_0 E_c J_g^{\mu}\ \exp(J_g/J_c)^{\mu}/(H_d^m T_p\mu_0 d^2)]^{1/(1+\mu)}. \tag{12}$$

This equation determines the temperature- field-, and criterion-dependent critical current density $J_c(T_p,H_d,E_c)$ completely. Keeping in mind that all the experimental fitting functions are obtained from studying the χ'' peak position, we write $T\equiv T_p$ hereafter for simplicity. For example, letting

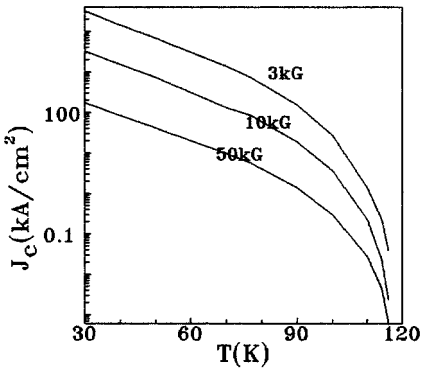

FIG. 10. The extrapolated $J_c(T)$ curves at $E_c=10^{-4}$ V/m and different fields based on Eq. (10).

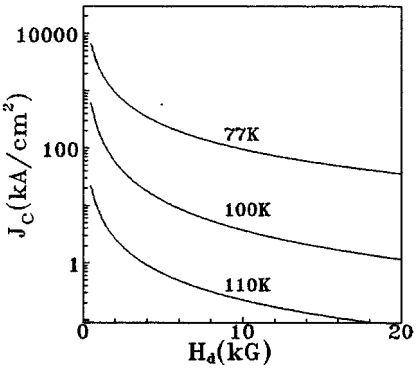

FIG. 11. The extrapolated $J_c(H_d)$ curves at $E_c=10^{-4}$ V/m and different temperatures based on Eq. (10).

$E_c=10^{-4}$ V/m and using $d=1$ μm $t_0=10^{-9}$ s, one can calculate the critical current densities at different H_d and T. Shown in Figs. 10 and 11 are the important $J_c(T)$ and $J_c(H_d)$ curves, respectively, which are obtained by extrapolating Eq. (12) to temperatures and fields where our experiment has not been carried out but which are interesting for scientific research and technical applications.

The stability of the flux-creep-determined J_c should be studied, and it has been determined by Eq. (10), e.g., as a result of the logarithmic decay, the normalized decay during one week $[J_c(t=1\ \text{week})/J_c(t=1\ \text{min})]$ is about 0.5 only, which means such flux-creep J_c values are rather stable. These results show that Hg-1223 phase material has high and stable J_c and is a promising material for applications.

IV. SUMMARY

The effective barrier U for flux diffusion, $U(J,H_d,T)=AJ^{-\mu}H_d^{-m}(1-T^r/T_c^r)^n$, and the critical current density $J_c(H_d,T,E_c)$ as a function of dc field, temperature, and criterion for Hg-1223 are obtained by systematic ACS measurements. The fundamental flux dynamics function, i.e., the activation barrier $U(J,H_d,T)$, current relaxation $J(t)$, magnetic J_c, the so-called irreversibility lines, and the characteristic curves E vs J determined by the earlier relaxation measurements (in the time window 10^{-5}–10^{-1} s) are compared with the predictions of the vortex glass and collective creep theories. The glassy exponent $\mu=0.43$ at $T\approx 110$ K and $J=10^2$ A/cm^2 is considered to be evidence of the charge-density-wave-type pinning and creep in the vortex glass phase predicted by the vortex glass and collective creep theories. The high J_c and high T_c indicate that the Hg-based compound is a promising material for technical applications.

ACKNOWLEDGMENTS

The authors thank L. Qiu and Professor Z. Yu for their help. This work was supported by the National Center for R&D on Superconductivity under Contract No. J-A-4102.

[1] S. N. Putilin, E. V. Antipov, O. Chmassem, and M. Marezio, Nature **362**, 226 (1993).
[2] A. Schilling, M. Cantoni, J. D. Guo, and H. R. Ott, Nature **363**, 56 (1993).
[3] S. N. Putilin, E. V. Antipov, and M. Marezio, Physica C **212**, 266 (1993).
[4] R. L. Meng, Y. Y. Sun, J. Kulik, Z. J. Huang, F. Chen, Y. Y. Xue, and C. W. Chu, Physica C **214**, 307 (1993).
[5] A. Schilling, O. Jeandupeux, J. D. Gao, and H. R. Ott, Physica C **216**, 6 (1993).
[6] U. Welp, G. W. Crabtree, J. L. Wagner, and D. G. Hinks, Physica C **218**, 373 (1993).
[7] J. Li, S. Y. Ding, H. M. Shao, J. S. Zhu, and Y. N. Wang, Physica C **232**, 10 (1994).
[8] Y. Rui, H. L. Ji, H. M. Shao, X. N. Xu, M. J. Qin, J. C. Shen, X. Jin, X. X. Yao, X. S. Rong, B. Ying, G. C. Che, and Z. H. Zhao, Physica C **231**, 243 (1994).
[9] Tomoichi Kamo, Toshiya Doi, Atsukoo Soeta, Toyotaka Yuasa, Naomi Inoae, Katsuzo Aihara, and Shi-pri Matsuda, Appl. Phys. Lett. **59**, 3186 (1991).
[10] S. Y. Ding, G. Q. Wang, X. X. Yao, H. T. Peng, Q. Y. Peng, and S. H. Chou, Phys. Rev. B **51**, 1091 (1995).
[11] J. Li, S. Y. Ding, H. M. Shao, J. S. Zhu, and Y. N. Wang, Physica C **235–240**, 3187 (1995).
[12] G. Blatter, M. N. Feigel'man, V. B. Geschkenbein, A. I. Larkin, and V. M. Vinokur, Rev. Mod. Phys. **66**, 1125 (1994).
[13] M. P. A. Fisher, Phys. Rev. Lett. **62**, 1415 (1989); D. S. Fisher, M. P. A. Fisher, and D. A. Huse, Phys. Rev. B **43**, 130 (1991).
[14] M. N. Feigel'man, V. B. Geshkenbein, A. I. Larkin, and V. M. Vinokur, Phys. Rev. Lett. **63**, 2303 (1989).
[15] J. R. Clem, in *Magnetic Susceptibility of Superconductors and Other Spin Systems*, edited by R. A. Hein, T. L. Francavila, and H. D. Liebenberg (Plenum, New York, 1992), pp. 177–211.
[16] K.-H. Muller, Physica C **168**, 585 (1990).
[17] S. Lofland, M. X. Huang, and S. M. Bhagat, Physica C **203**, 271 (1992).
[18] S. D. Murphy, K. Renouard, R. Crittenden, and S. M. Bhagat, Solid State Commun. **69**, 367 (1989).
[19] A. P. Malozemoff and M. P. A. Fisher, Phys. Rev. B **42**, 6784 (1991).